

Are Diamond Nanoparticles Cytotoxic?

Amanda M. Schrand,[†] Houjin Huang,[†] Cataleya Carlson,[‡] John J. Schlager,[‡] Eiji Ōsawa,^{§,||}
Saber M. Hussain,^{*,‡} and Liming Dai^{*,†}

Department of Chemical and Materials Engineering, University of Dayton, 300 College Park, Dayton, Ohio 45469-0240, Applied Biotechnology Branch, Human Effectiveness Directorate, Air Force Research Laboratory, Wright-Patterson AFB, Ohio 45433-5707, and NanoCarbon Research Institute, Ltd., Kashiwa-no-ha, Chiba 277-0882, Japan

Received: September 28, 2006; In Final Form: November 15, 2006

Finely divided carbon particles, including charcoal, lampblack, and diamond particles, have been used for ornamental and official tattoos since ancient times. With the recent development in nanoscience and nanotechnology, carbon-based nanomaterials (e.g., fullerenes, nanotubes, nanodiamonds) attract a great deal of interest. Owing to their low chemical reactivity and unique physical properties, nanodiamonds could be useful in a variety of biological applications such as carriers for drugs, genes, or proteins; novel imaging techniques; coatings for implantable materials; and biosensors and biomedical nanorobots. Therefore, it is essential to ascertain the possible hazards of nanodiamonds to humans and other biological systems. We have, for the first time, assessed the cytotoxicity of nanodiamonds ranging in size from 2 to 10 nm. Assays of cell viability such as mitochondrial function (MTT) and luminescent ATP production showed that nanodiamonds were not toxic to a variety of cell types. Furthermore, nanodiamonds did not produce significant reactive oxygen species. Cells can grow on nanodiamond-coated substrates without morphological changes compared to controls. These results suggest that nanodiamonds could be ideal for many biological applications in a diverse range of cell types.

With the recent development in nanoscience and nanotechnology, carbon-based nanomaterials (e.g., fullerenes, nanotubes, nanodiamonds) are receiving much attention due to their remarkable mechanical, electrical, and thermal properties.^{1–3} The importance of carbon nanomaterials in biological applications has been recently recognized. Examples include their potential uses in drug, gene, and protein delivery; novel imaging methods, coatings for implantable/corrosion resistant materials; biosensors/biochips; purification of proteins; medical nanorobots; and many other emerging biomedical technologies.^{4–9} In particular, carbon nanomaterials have recently been examined with both *in vivo* studies^{10–11} and *in vitro* cell cultures.^{12–18} Although the scientific community has been so far primarily focused on the potential biological applications of fullerenes and/or carbon nanotubes, other carbon nanomaterials (especially nanodiamonds) are beginning to emerge as alternative candidates for similar and many other applications. Both carbon nanotubes and nanodiamonds can be similarly modified for nanocomposite and biological applications.¹⁹ It is envisaged that nanodiamonds may prove to be an even better drug carrier, imaging probe, or implant coating in biological systems compared to currently used nanomaterials due to its optical transparency, chemical inertness,

high specific area, and hardness.^{4,20} Recent progresses in the dispersion of detonation nanodiamonds (NDs, 2–10 nm) in aqueous media made by Ōsawa and co-workers has facilitated the use of NDs in physiological solutions,²¹ whereas most previous studies have focused on polycrystalline chemical vapor deposited (CVD) diamond films for biomedical applications.^{6,7,22} It has been recognized that a bulk material with good biocompatibility may not be as well-tolerated by the body once it is in a fine particulate or nanometer-sized form. Although the CVD diamond thin films are generally regarded as biologically inert, noninflammatory, and biocompatible, are diamond nanoparticles also well tolerated by cells? The availability of the newly produced detonation NDs in aqueous dispersed forms facilitates their possible use in nanomedicine (e.g., medical nanorobots made of NDs) and biorelated studies.³ However, the environmental impact of the detonation NDs, especially on humans and other biological systems, has not been properly studied.

In one recent study, Yu et al. investigated the biocompatibility of relatively large synthetic abrasive diamond powders (100 nm) in cell culture and found very low cytotoxicity in kidney cells.⁵ These authors visualized their diamond nanoparticles with fluorescent confocal microscopy to enter the cells and localize in the cytoplasm. For these nanodiamonds to be fluorescent, however, these authors performed the tedious procedures of electron beam irradiation and annealing of the nanoparticles. At the nanometer scale, the particle properties depend strongly on the size of the material.³ As a consequence, changes in the size-dependent cytotoxicity may be observed for diamond nanoparticles of different sizes. Due to the high surface-to-

* Corresponding authors. L.D.: tel, 937-229-2670; Fax: 937-229-3433; e-mail, ldai@udayton.edu. S.H.: tel, 937-904-9517; fax, 937-904-9610; e-mail, saber.hussain@wpafb.af.mil.

[†] University of Dayton.

[‡] Wright-Patterson AFB.

[§] NanoCarbon Research Institute, Ltd..

^{||} Present address: Asama Research Extension Centre, Shinshu University, 3-15-1 Tokita, Ueda, 386-8567, Japan.

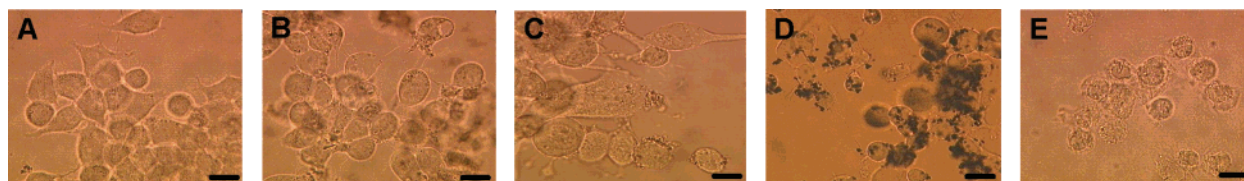


Figure 1. Incubation of cells with various nanoparticle concentrations after 24 h viewed with light microscopy: (A) control; (B) 100 $\mu\text{g}/\text{mL}$ ND-raw; (C) 100 $\mu\text{g}/\text{mL}$ ND-COOH; (D) 100 $\mu\text{g}/\text{mL}$ CB; (E) 2.5 $\mu\text{g}/\text{mL}$ CdO. Note that nanoparticles are seen surrounding the cell borders and attached to neurite extensions whereas cell morphology is unaffected by the presence of nanodiamonds. Scale bars are 20 μm .

volume ratio associated with nanometer-sized materials, a tremendous surface chemistry effect on the nanoparticle properties is also expected.³ Previous studies in our AFB laboratory have primarily concerned metal nanoparticle toxicity using *in vitro* cell culture models for chemical toxicity screening.^{23–28} In the present study, we report the first biocompatibility study of small NDs (2–10 nm), synthesized by the detonation of carbon-containing explosives in an inert atmosphere,^{21,29} and possible effects of the surface chemistry by treating the NDs with acids or bases ($-\text{COOH}$, $-\text{COONa}$, $-\text{SO}_3\text{Na}$; see Supporting Information). In conjunction with tests to determine cytotoxicity, cells were grown on ND-coated substrates to examine their interactions and sustained viability over time.

Nanodiamonds were generously supplied by NanoCarbon Research Institute Ltd. and were synthesized according to previously reported detonation techniques.^{21,29} Nanometer-sized carbon black (CB, Cabot) and submicron-sized cadmium oxide (CdO, Fluka Chemical Co.) were used as negative and positive controls, respectively. All nanoparticles were UV-sterilized and then diluted to a stock concentration of 1 mg/mL in deionized water. Characterization of nanoparticle size and morphology was performed with transmission electron microscopy (TEM, Hitachi H-7600 W-tip). The chemical nature of the functionalized NDs was examined with X-ray photoelectron spectroscopy (VG Microtech ESCA 2000) using monochromatic Mg K α radiation at a power of 300 W, Fourier transformed infrared spectroscopy (FTIR, Perkin-Elmer, Spectrum One) and Raman spectroscopy (Renishaw, inVia reflex microRaman, 514.5 nm laser). ND substrates were prepared by drop casting solutions of ND onto collagen or poly(L-lysine) coated glass coverslips and drying for 1 h under UV light before plating cells.

Neuroblastoma cells, a neuronal phenotype, were generously provided by Dr. David Cool's laboratory at Wright State University (Dayton, OH) and other cells were purchased from the American Type Culture Collection (ATCC). All cells were plated and grown according to standard cell culture techniques.²⁶ After a desired growth period, cell cultures were dosed with freshly prepared nanoparticle working solutions at concentrations ranging between 5 and 100 $\mu\text{g}/\text{mL}$ in cell culture media without serum. pH values were controlled between 7.2 and 7.6 for both control dosing media and nanoparticles in the cell culture solutions. Fluorescent microscopy was performed to examine mitochondrial membrane permeability (Rhodamine 123, JC-1, Invitrogen and Mit $-\text{E}-\Psi$ membrane permeability detection kit, BioMol). Both mitochondrial dyes entered the live cells after 15–30 min at 37 $^{\circ}\text{C}$. If the mitochondrial membranes have been damaged after incubation with nanoparticles, then the dyes will disperse in the cytoplasm due to leakage, whereas intact mitochondrial membranes will retain and aggregate the dye. Fluorescence was visualized with TRITC and FITC filters on an Olympus IX71 epifluorescent microscope. Nanoparticle-treated cell samples for TEM study were fixed with glutaraldehyde/paraformaldehyde, stained with osmium tetroxide, dehydrated through analytical grade ethanol, embedded in resin, cured, and thin sectioned. For scanning electron microscopy

(SEM, Hitachi S-4800), cells were first fixed and dehydrated as described above, mounted to aluminum stubs with double-sided carbon adhesive tape, and then air-dried and sputter-coated with gold.

The 3-[4,5-dimethylthiazol-2-yl]-2,5-diphenyltetrazolium bromide (MTT) assay was conducted to assess cellular viability based on mitochondrial function³⁰ with a slight modification of removing nanoparticles with centrifugation before microplate reading (*vide infra*). After 30 min of incubation with MTT, a purple color developed within the cells, indicating the cleavage of the tetrazolium salt (MTT) by mitochondrial reductase in live cells. The purple product (formazan crystals) was extracted into solution for homogeneous staining and the absorbance was read on a Spectromax 190 microplate reader at 570–630 nm. The percent reduction of MTT was compared to controls (cells not exposed to nanoparticles), which represented 100% MTT reduction. The CellTiter-Glo luminescent viability assay was performed to reconfirm data from the MTT assay. This assay provides a homogeneous method for determining the number of viable cells in culture based on quantitation of adenosine 5' triphosphate (ATP), which indicates the presence of metabolically active cells.

Oxidative stress was measured in relation to the generation of reactive oxygen species (ROS). Prior to dosing cells with nanoparticles, the fluorescent probe 2',7'-dichlorofluorescein diacetate (DCHF-DA, Sigma) was applied under a light controlled environment as described by Wang and Joseph.³¹ After nanoparticle treatment, the fluorescent intensity from each well was measured with a 485 nm excitation filter and a 530 nm emission filter on a SpectraMAX Gemini Plus microplate reader (Molecular Device) equipped with SOFTmax Pro 3.1.2 software (Molecular Devices Corp., Sunnyvale, CA). The positive control, hydrogen peroxide (30% H_2O_2 , Fisher Scientific), was used to assess the reactivity of the probe. Biochemical assays (MTT and ROS) were done in triplicate and the results were presented as mean \pm standard deviation.

All nanoparticles in this study have average sizes ranging from 2 to 10 nm for nanodiamonds (ND), 20–30 nm for nanometer-sized CB, and up to hundreds of nanometers for cadmium oxide (CdO). Characterization of nanoparticle size distributions and morphologies was accomplished with transmission electron microscopy (TEM; see Supporting Information). The morphology of neuroblastoma cells was round immediately after trypsinization. Upon attachment and growth, however, some of the cells developed elongated extensions and others remained round, which is characteristic of these cells. For morphological examination of cell–nanoparticle interactions, cells were incubated with media alone (control) or media containing nanoparticles at various concentrations. After 24 h of incubation with NDs or CB nanoparticles, cells appeared similar to control cells with some cells displaying an elongated morphology (Figure 1A–D). The ND and CB were irregularly shaped particles in the surrounding media, agglomerated at cell borders, along their processes, and within the cells at concentrations ranging from 5 to 100 $\mu\text{g}/\text{mL}$ (Figure 1A–D). In contrast,

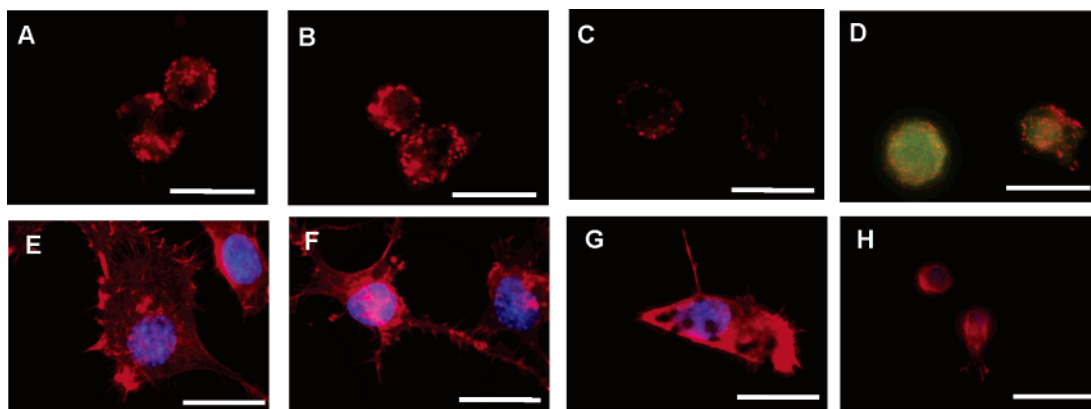


Figure 2. Fluorescent microscopy of neuroblastoma cells incubated with or without nanoparticles for 24 h with Mito-E-Ψ stains for mitochondrial membrane permeability detection (A)–(D) or dual actin/nuclear staining to examine changes in cytoskeletal architecture (E)–(H): (A), (E) control; (B), (F) 100 $\mu\text{g/mL}$ ND-raw; (C), (G) 100 $\mu\text{g/mL}$ CB; (D), (H) 2.5 $\mu\text{g/mL}$ CdO. Note that the cells incubated without nanoparticles or with nanodiamonds showed intact mitochondrial membranes whereas cells incubated with carbon black or CdO may have been damaged after nanoparticle exposure, indicative of mitochondrial membrane leakage and the initiation of apoptosis. Additionally, NDs appear to increase neurite outgrowth and branching. Scale bars are 10 μm .

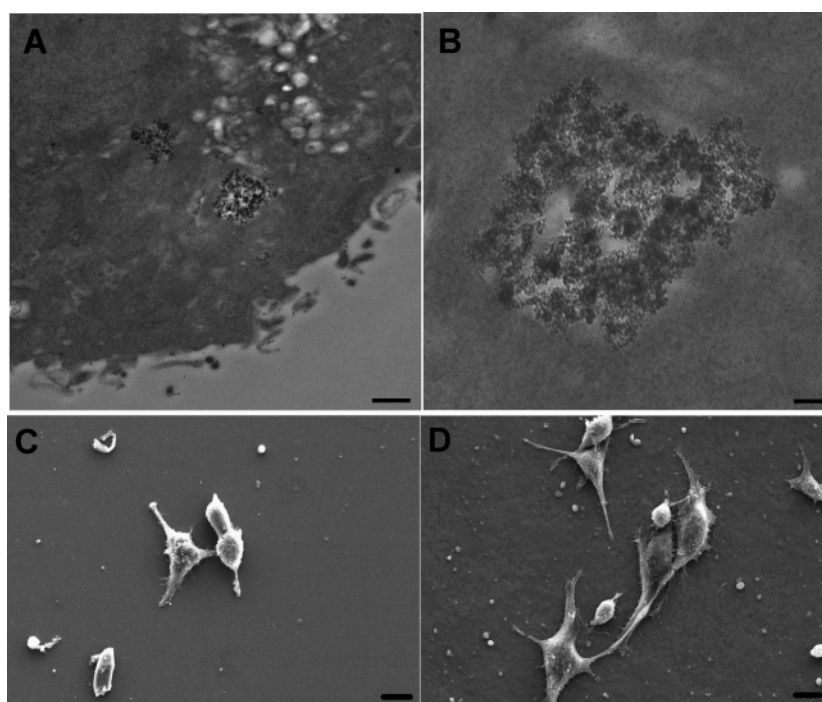


Figure 3. Interaction of neuroblastoma cells with nanodiamonds. (A) TEM image showing internalized nanodiamonds after exposure to 25 $\mu\text{g/mL}$ ND-COOH for 24 h. (B) Higher magnification of lower agglomerate in (A). (C) SEM image of cell growth on a control collagen substrate after 6 h. (D) SEM image of cells grown on a ND-COOH coated collagen substrate after 96 h. Scale bars are (A) 500 nm, (B) 100 nm, and (C), (D) 10 μm .

cells incubated with the positive control CdO (Figure 1E) lacked cellular extensions, were reduced in size, had irregular cell borders, and formed vacuoles, which are morphological indicators of toxicity. For simplicity, only images of the highest concentrations of ND-raw and ND-COOH (100 $\mu\text{g/mL}$) are included to represent unfunctionalized and acid-functionalized NDs, respectively. Base-functionalized NDs, ND-SO₃Na and ND-COONa, displayed similar morphological characteristics to ND-raw and ND-COOH. Additionally, only a low concentration (2.5 $\mu\text{g/mL}$) of CdO was shown to demonstrate its strong toxicity.

To further examine interactions between the cells and nanoparticles, changes in mitochondrial membrane permeability and cytoskeletal architecture were examined with fluorescent microscopy (Figure 2). The Mito-E-Ψ fluorescent reagent, when aggregated inside healthy mitochondria, fluoresces red whereas

dispersion of the dye due to mitochondrial membrane disruption causes it to fluoresce green in the cytoplasm. Aggregation and retention of the mitochondrial dye inside healthy cells was shown in control cells (Figure 2A), cells incubated with 100 $\mu\text{g/mL}$ ND-raw (Figure 2B), and to a lesser extent in cells incubated with 100 $\mu\text{g/mL}$ CB (Figure 2C). Cells incubated with CB had noticeable dark CB nanoparticles attached to cell borders or internalized, which tended to block the fluorescent signal in certain areas compared to cells incubated with NDs (Figure 2C). The dispersion of the dye was apparent in cells treated with 2.5 $\mu\text{g/mL}$ CdO, suggesting toxicity and the initiation of apoptosis or programmed cell death (Figure 2D). Therefore, these results show that the mitochondrial membrane was clearly maintained in cells incubated with ND in support of the biocompatibility of NDs. In the case of cytoskeletal alterations after incubation with NDs, distinct branching and extension of

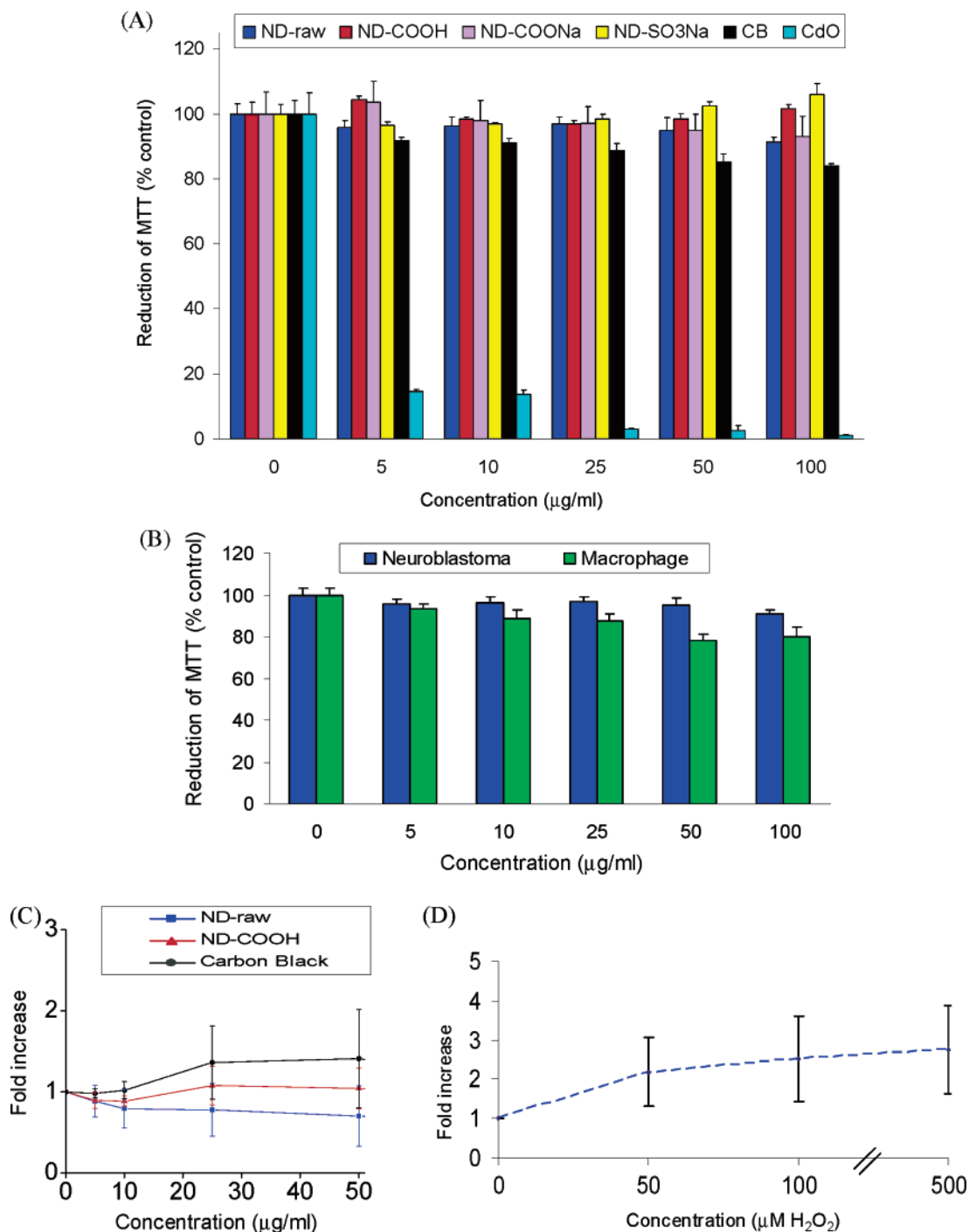


Figure 4. Cytotoxicity evaluation of cells incubated with various nanoparticles for 24 h. (A) Mitochondrial function of neuroblastoma cells determined by the reduction of MTT after nanoparticles were removed by centrifugation. (B) Similar reductions in MTT for neuroblastoma cells and macrophages (ND-raw). (C) Generation of reactive oxygen species (ROS) from neuroblastoma cells determined by the hydrolysis of DCHF-DA after 24 h of incubation with various nanoparticles (ND-raw, ND-COOH, and CB). (D) Positive control hydrogen peroxide induces ROS production.

multiple neurites was found after 24 h (Figure 2F) compared to control (Figure 2E), CB (Figure 2G), or CdO (Figure 2H) treated cells. Again, noticeable black CB nanoparticles could be seen attached to the cells (Figure 2G) or cell shrinkage due to the toxic effects of CdO (Figure 2H).

Because individual NDs were too small to be resolved inside the cells with conventional light or fluorescent microscopy, the internalization of NDs into the cells after 24 h was examined with TEM. As can be seen in Figure 3A,B, NDs were found inside the cells after incubation with 25 $\mu\text{g/mL}$ of ND-COOH for 24 h. Although these representative images do not specify the exact location of the ND particles, they appear to localize

in the cytoplasm in aggregates approximately 500 nm in size (Figure 3A,B). Although the internalization of nanodiamonds into the cells could provide new nanotherapeutics with the nanodiamonds as biological transporters^{32–34} or internalized cell killers,³⁵ as is the case of carbon nanotubes, they may be difficult to clear from the cell. The possible long-term pathologic effects of the internalized nanodiamonds on the cells and the related long-term and acute toxicology data on the animal model are still pending for further investigation.

Additionally, cells were plated on ND substrates to determine if they could adhere and grow while maintaining morphologies similar to control cells. After 96 h, cells grown on the ND-

COOH coated collagen substrates (Figure 3D) were viable with morphologies similar to control cells (Figure 3C), suggesting that these substrates allow cell attachment and growth.

To more quantitatively determine the toxicity or biocompatibility of NDs, colorimetric (MTT), luminescent (Cell-titer Glo), and fluorescent (ROS) assays were performed. The MTT assay was selected to assess the mitochondrial function of neuroblastoma cells. Mitochondria are vulnerable targets for toxic injury by a variety of compounds because of their crucial role in maintaining cellular structure and function via aerobic ATP production.²⁴ The reduction of MTT dye occurs only in functional mitochondria, therefore, a decrease in MTT dye reduction is an indication of damage to mitochondria. CdO exhibited strong toxicity with its capability to sharply decrease cell viability, compared to the control, leading to a strong concentration dependence over the whole concentration range from 5 to 100 $\mu\text{g/mL}$ (Figure 4A). Nanometer-sized carbon black showed slightly reduced cell viability, but no significant difference from controls at concentrations up to 100 $\mu\text{g/mL}$. However, cells incubated with various concentrations of functionalized or unfunctionalized nanodiamonds had some slightly higher values, but again no significant difference in viability compared to controls at concentrations up to 100 $\mu\text{g/mL}$ (Figure 4A). To further confirm the low cytotoxicity of NDs, three other cells types (macrophages, keratinocytes, and PC-12 cells) were investigated and found to display similar trends of low cytotoxicity. A comparison between neuroblastoma cells and macrophages demonstrated that NDs display no toxicity even to cells, which may have different methods of internalization (Figure 4B).

To further verify the biocompatibility of nanodiamonds, we measured luminescence, corresponding to ATP production, as a marker of cell viability (see Supporting Information). Similar trends for nanoparticle toxicity were found, but surprisingly, the luminescence value for ND-raw was lower than nanometer-sized CB, though these values were not significantly different from the control. It is worthwhile to point out here that our recent work (see Supporting Information), along with others,⁴ has indicated that nanoparticles could interfere with various colorimetric cytotoxicity assays, such as the MTT and CellTiter-Glo luminescent viability assays, probably due to light scattering and/or direct nanoparticle interaction with the chemical components of the assays. All data in Figure 4A,B were taken after the incorporation of an additional centrifugation step to remove the nanoparticles from the plate before reading.

To investigate nanoparticle-induced oxidative stress as mechanistic changes, we assessed the generation of reactive oxygen species (ROS).³⁶ ROS are naturally generated byproducts of cellular redox/enzymatic reactions such as mitochondrial respiration, phagocytosis, and metabolism. However, they can also unregulate generation, leading to a condition known as oxidative stress, which can cause numerous pathological conditions.³⁷ Increases in intracellular ROS (oxidative stress) represent a potentially toxic insult which, if not neutralized by antioxidant defenses (e.g., glutathione and antioxidant enzymes) could lead to membrane dysfunction, protein degradation, and DNA damage.^{38–42}

The fluorescence intensity of dichlorofluorescein (DCF), an oxidized form of 2',7'-dichlorofluorescein, can be used as a measure of the cumulative production of ROS over a period of nanoparticle exposure. We found that CB shows a higher level of ROS production than ND (Figure 4C). The positive control for this assay, hydrogen peroxide (H_2O_2), showed a dose-dependent increase in ROS production (Figure 4D). The

relatively low level of ROS generation produced in cells incubated with NDs is consistent with the MTT and ATP results. Therefore, these results further support the biocompatibility of NDs and suggest that ND does not induce ROS generation in this *in vitro* cell model system.

In summary, we have demonstrated that 2–10 nm nanodiamonds, with and without surface modification by acid or base, are biocompatible with a variety of cells of different origins, including neuroblastoma, macrophage, keratinocyte, and PC-12 cells. Several methods for assessing toxicity were used to rigorously test the cytotoxicity of the nanodiamonds (2–10 nm) using carbon black (20–30 nm) and cadmium oxide (100–1000 nm) as negative and positive controls, respectively. Although the cell types used may have different mechanisms of internalization of the nanodiamonds and the long-term effect of the internalized nanodiamonds on the cells needs to be further investigated, the resultant retention of mitochondria membrane along with low levels of ROS suggests that once inside the cell the nanodiamonds remain nonreactive. In conjunction with the toxicity testing of nanodiamonds, cells were grown on ND-coated substrates to examine their interactions and sustained viability over time, which provided further assurance for the utility of nanodiamonds as biologically compatible materials.

Acknowledgment. We thank Col. J. Riddle for his strong support and encouragement for this research. TEM work was performed at the Nanoscale Engineering Science and Technology Laboratory (NEST), University of Dayton. A.S. is funded by the Biosciences and Protection Division, Air Force Research Laboratory, under the Oak Ridge Institute for Science and Education, Oak Ridge, TN, and the Dayton Area Graduate Studies Institute (DAGSI). L.D. and E.O. thank NEDO International Cooperative Grant (2004IT081) for financial support.

Supporting Information Available: Experimental details for nanoparticle characterization, nanoparticle interference assays, and bacterial growth in nanodiamond-containing solutions. This material is available free of charge via the Internet at <http://pubs.acs.org>.

References and Notes

- Baughman, R. H.; Zakhidov, A. A.; de Heer, W. A. *Science* **2002**, *297*, 787–792.
- Zhang, M.; Fang, S.; Zakhidov, A. A.; Lee, S. B.; Aliev, A. E.; Williams, C. D.; Atkinson, K. R.; Baughman, R. H. *Science* **2005**, *309*, 1215–1219.
- Dai, L., Ed. *Carbon Nanotechnology: Recent Developments in Chemistry, Physics, Materials Science and Device Applications*; Elsevier: Amsterdam, 2006.
- Huang, L.-C. L.; Chang, H.-C. *Langmuir* **2004**, *20*, 5879–5884.
- Yu, S. J.; Kang, M.-W.; Chang, H.-C.; Chen, K.-M.; Yu, Y.-C. *J. Am. Chem. Soc.* **2005**, *127*, 17604–17605.
- Yang, W.; Auciello, O.; Butler, J. E.; Cai, W.; Carlisle, J. A.; Gerbi, J. E.; Gruen, D. M.; Knickerbocker, T.; Lassetter, T. L.; Russell, Jr., J. R.; Smith, L. M.; Hamers, R. J. *Nat. Mater.* **2002**, *1*, 253–257.
- Poh, W. C.; Loh, K. P.; Zhang, W. D.; Triparthy, S.; Ye, J.-S.; Sheu, F.-S. *Langmuir* **2004**, *20*, 5484–5492.
- Bondar, V.; Pozdnyakova, I. O.; Puzyr, A. P. *Phys. Solid State* **2004**, *46*, 758–760.
- Pantarotto, D.; Briand, J.-P.; Prato, M.; Bianco, A. *Chem. Commun* **2004**, 16–17.
- Muller, J.; Huaux, F.; Moreau, N.; Misson, P.; Heilier, J.-F.; Delos, M.; Arras, M.; Fonseca, A.; Nagy, J. B.; Lison, D. *Toxicol. Appl. Pharmacol.* **2005**, *207*, 221–231.
- Gharb, N.; Pressac, M.; Hadchouel, M.; Szwarc, H.; Wilson, S. R.; Moussa, F. *Nano Lett.* **2005**, *5*, 2578–2585.
- Ding, L.; Stilwell, J.; Zhang, T.; Elboudwrej, O.; Jiang, H.; Selegue, J. P.; Cooke, P. A.; Gray, J. W.; Chen, F. F. *Nano Lett.* **2005**, *5*, 2448–2464.
- Cui, D.; Tian, F.; Ozkan, C. S.; Wang, M.; Gao, H. *Toxicol. Lett.* **2005**, *155*, 73–85.

- (14) Monteiro-Riviere, N. A.; Nemanich, R. J.; Inman, A. O.; Wang, Y. Y.; Riviere, J. E. *Toxicol. Lett.* **2005**, *155*, 377–384.
- (15) Manna, S. K.; Sarkar, S.; Barr, J.; Wise, K.; Barrera, E. V.; Jejelowo, O.; Rice-Ficht, A. C.; Ramesh, G. T. *Nano Lett.* **2005**, *5*, 1676–1684.
- (16) Sayes, C. M.; Liang, F.; Hudson, J. L.; Mendez, J.; Guo, W.; Beach, J. M.; Moore, V. C.; Doyle, C. D.; West, J. L.; Billups, W. E.; Ausman, K. D.; Colvin, V. L. *Toxicol. Lett.* **2005**, *161*, 135–142.
- (17) Soto, K.; Carrasco, A.; Powell, T.; Garza, K.; Murr, L. *J. Nanopart. Res.* **2005**, *7*, 145–169.
- (18) Special issue. *Carbon* **2006**, *44*, No. 6 (May), 1027–1120.
- (19) (a) Osswald, S.; Yushin, G.; Mochalin, V.; Kucheyev, S. O.; Gogotsi, Y. *J. Am. Chem. Soc.* **2006**, *128*, 11635–11642. (b) Khabashesku, V. N.; Margrave, J. L.; Barrera, E. V. *Diamond Relat. Mater.* **2005**, *14*, 859–866.
- (20) Shenderova, O. A.; Zhirnov, V. V.; Brenner, D. W. *Crit. Rev. Solid State Mater. Sci.* **2002**, *27*, 227–356.
- (21) Kruger, A.; Kataoka, F.; Ozawa, M.; Fujino, T.; Suzuki, Y.; Aleksenskii, A. E.; Vul', A. Ya.; Osawa, E. *Carbon* **2005**, *43*, 1722–1730.
- (22) Huang, T. S.; Tzeng, Y.; Liu, Y. K.; Chen, Y. C.; Walker, K. R.; Guntupalli, R.; Liu, C. *Diamond Rel. Mater.* **2004**, *13*, 1098–1102.
- (23) Trohalaki, S.; Zellmer, R. J.; Pachter, R.; Hussain, S. M.; Frazier, J. M. *Toxicol. Sci.* **2002**, *68*, 498–507.
- (24) Hussain, S. M.; Frazier, J. M. *Toxicol. Sci.* **2002**, *69*, 424–432.
- (25) Hussain, S. M.; Frazier, J. M. *Toxicol. In Vitro* **2003**, *17*, 343–355.
- (26) Hussain, S. M.; Hess, K. L.; Gearhart, J. M.; Geiss, K. T.; Schlager, J. J. *Toxicol. In Vitro* **2005**, *19*, 975–983.
- (27) Hussain, S. M.; Frazier, J. M. *Sci. Total Environ.* **2001**, *274*, 151–160.
- (28) Braydich-Stolle, L.; Hussain, S.; Schlager, J. J.; Hofmann, M. *Toxicol. Sci.* **2005**, *88*, 412–419.
- (29) Greiner, N. R.; Phillips, D. S.; Johnson, J. D.; Volk, F. *Nature* **1988**, *333*, 440–442.
- (30) Carmichael, J.; DeGraff, W. D.; Gazdar, A. F.; Minna, J. B.; Mitchell, J. *Cancer Res.* **1987**, *47*, 936–942.
- (31) Wang, H.; Joseph, J. A. *Free Radical Biol. Med.* **1999**, *27*, 612–616.
- (32) Pantaarotto, D.; Briand, J.-P.; Prato, M.; Bianco, A. *Chem. Commun.* **2004**, 16–17.
- (33) Kostarelos, K.; Lacerda, L.; Partidos, C. D.; Prato, M.; Blanco, A. *J. Drug Delivery Sci. Technol.* **2005**, *15*, 41–47.
- (34) Kam, N. W. S.; Jessop, T. C.; Wender, P. A.; Dai, H. *J. Am. Chem. Soc.* **2004**, *126*, 6850–6851.
- (35) Kam, N. W. S.; O'Connell, M.; Wisdom, J. A.; Dai, H. *J. Proc. Natl. Acad. Sci.* **2005**, *102*, 11600–11605.
- (36) Nel, A.; Xia, T.; Madler, L.; Li, N. *Science* **2006**, *311*, 622–627.
- (37) Farber, J. L.; Kyle, M. E.; Coleman, J. B. *Lab. Invest.* **1990**, *62*, 670–679.
- (38) Preece, N. E.; Timbrell, J. A. *J. Pharmacol. Toxicol.* **1989**, *64*, 282–285.
- (39) Loft, S.; Poulsen, H. E. *Methods Enzymol.* **1999**, *300*, 166–184.
- (40) Halliwell, B.; Gutteridge, J. M.; Cross, C. E. *J. Lab. Clin. Med.* **1992**, *119*, 598–620.
- (41) Yu, B. P. *Physiol. Rev.* **1994**, *74*, 139–162.
- (42) Siesjo, B. K.; Agardh, C. D.; Bengtsson, F. *Cerebrovasc. Brain Metab. Rev.* **1989**, *1*, 165–211.